

Short communication

## Current collecting efficiency of micro tubular SOFCs

Toshio Suzuki\*, Toshiaki Yamaguchi, Yoshinobu Fujishiro, Masanobu Awano

*Advanced Manufacturing Research Institute, National Institute of Advanced Industrial Science and Technology (AIST),  
2266-98 Anagahora, Shimo-shidami, Moriyama-ku, Nagoya 463-8560, Japan*

Received 25 August 2006; received in revised form 19 September 2006; accepted 21 September 2006

Available online 13 November 2006

### Abstract

In this study, current collecting efficiency of the micro tubular solid oxide fuel cell (SOFC) was estimated to determine optimum size of the micro tubular SOFC. Two models for collecting current from single terminal (ST) and double terminal (DT) of anode tube were proposed and used to calculate the current collecting efficiency as functions of anode thickness, tube length and operating temperature. It was shown that design of the cell geometry and current correcting method are significantly important to achieve high performance micro tubular SOFC stacks. The efficiency loss estimated from the DT model was about 2–4-fold lower than those of obtained from the ST model. The DT model was shown to be more effective for higher operating temperature and the tube length.

© 2006 Elsevier B.V. All rights reserved.

**Keywords:** Current collection; Model; Tubular SOFCs; Micro SOFC

### 1. Introduction

Intermediate temperature operation of solid oxide fuel cell (SOFC) system is expected to decrease material degradation and prolong stack life time, reduce cost by utilizing metal materials [1,2]. In recent years, several groups have reported outstanding cell performance with power densities of 0.8–2 W cm<sup>-2</sup> at 600 °C or under using planar anode-supported SOFCs with thin film electrolytes, doped CeO<sub>2</sub> or doped LaGaO<sub>3</sub> [3–5]. Therefore, SOFC is becoming more realistic option for the energy sources of the next generation. To accelerate commercialization of SOFCs as power sources especially for portable devices and auxiliary power units for automobile, it is important to develop high efficient small cell stacks, which are robust for rapid temperature control.

Micro tubular SOFC systems have shown many desirable characteristics over planar SOFC systems [6–10]. It was shown that small-scale tubular SOFCs endured thermal stress caused by rapid heating up to operating temperature. It is also possible to design SOFC stacks with high volumetric power density by using micro tubular SOFCs with 2 mm or less diameter. For

example, a tubular cell with 1.6 mm diameter and 1 cm length could have electrode area of about 0.5 cm<sup>2</sup>. In 1 cm<sup>3</sup>, 25 (5 × 5) cells can be placed, in which total electrode area sums up to over 12 cm<sup>2</sup>.

A key to develop such micro cells lies in development of electrolyte/electrode materials that enable lower-temperature SOFC operation and of manufacturing process technologies integrating and arranging such micro cells, as well as controlling microstructure of the electrodes. This research (Advanced Ceramic Reactor Project) aims to realize high-efficient ceramic reactors that are operable at intermediate temperature range (under 650 °C) and possibly generate more than 2 kW/liter of high power density applicable to the auxiliary power unit (APU), etc., by improvement of materials, accumulation of fine parts, and assembly of them as a high performance module. Thus, development of advanced ceramic reactors is expected to accelerate the commercialization of SOFC systems.

After 1 year of this project, we have successfully fabricated micro tubular SOFCs and demonstrated their excellent performance, generation of power density  $\sim 1$  W cm<sup>-2</sup> at 570 °C by applying ceramic processing techniques developed in this study. Furthermore, development of novel ceramic fabrication processes for integration of SOFCs in a cube stack and accumulation of cubes as a prototype module is on progress. In

\* Corresponding author. Tel.: +81 52 736 7299; fax: +81 52 736 7405.  
E-mail address: [toshio.suzuki@aist.go.jp](mailto:toshio.suzuki@aist.go.jp) (T. Suzuki).

addition, 3D micro honeycomb type cell stacks have been fabricated with cell integration density of 100 tubes or more per 1 cm<sup>3</sup>.

For further development of the micro tubular SOFC stacks, proper current collecting method needs to be addressed, since selection of current collecting method becomes critical to achieve reasonable fuel efficiency as the size of the cell decreases. In this study, two anode current collecting methods were proposed to estimate efficiency loss due to anode tube resistance as a current collector. The results of the calculation are expected to use to optimize the size (thickness and length of anode tube) of the micro tubular SOFCs.

### 2. Experimental

The cells prepared in this study consist of 70 wt% NiO–Gd doped ceria (GDC) as an anode (support tube), GDC as an electrolyte and 70 wt% (La, Sr)(Fe, Co)O<sub>3</sub> (LSCF)–GDC as a cathode. Details for preparation were reported elsewhere [11]. Microstructure of the anode tube was investigated using SKYSCAN 1172.

The performance of the cell was investigated using a Solartron 1260 frequency response analyzer with a 1296 interface using 4-probe configuration. The size of the cell was 1.6 mm diameter and 1 cm length with active cathode length (*L*) of 7 mm, whose active cell area is 0.35 cm<sup>2</sup>. 20 vol% humidified H<sub>2</sub> (3% H<sub>2</sub>O) in N<sub>2</sub> was used as a fuel in the flow rate of 25 cc min<sup>-1</sup>. The Ag wire was used for collecting current, which was fixed using Ag paste on the cathode and anode.

### 3. Model

To estimate the efficiency of current collection from the anode tube, two following models were used in this study as shown

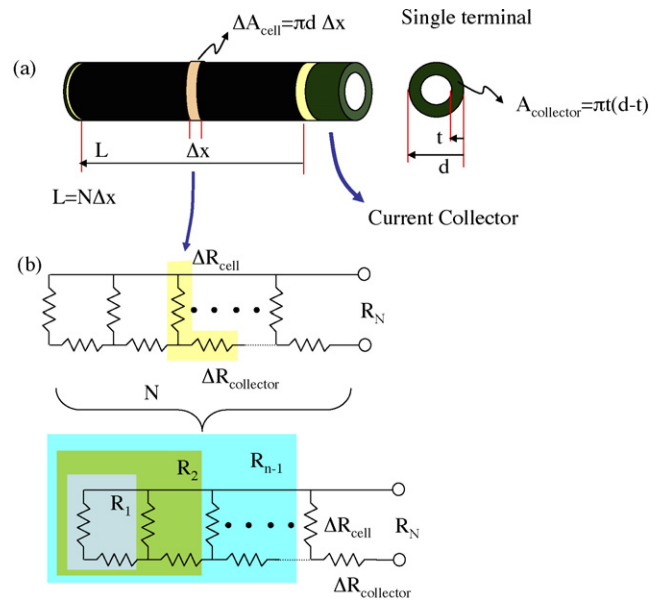


Fig. 1. (a) Schematic image of the single terminal current collecting method. (b) A model equivalent circuit for the single terminal current collection.

in Figs. 1 and 2, namely single and double terminal current collecting methods, respectively.

#### 3.1. Single terminal (ST) model

Fig. 1(a) shows the schematic image of single terminal (ST) current collecting method. Current collection from the anode side is only made from single terminal of the anode tube, while whole area of the cathode was used for current collection from the cathode side. The anode tube (length,  $L$ ; diameter,  $d$ ; tube thickness,  $t$ ) was divided into  $N$  and each of them was assigned to an equivalent circuit (highlighted in Fig. 1(b)).  $R_1, R_2, \dots,$

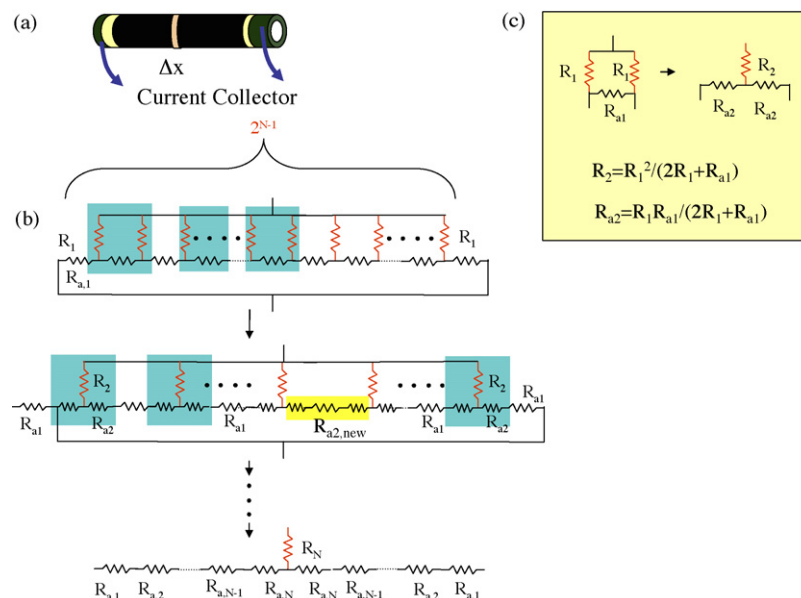


Fig. 2. (a) Schematic image of the double terminal current collecting method. (b) A model equivalent circuit for the double terminal current collection. (c) The formula of  $\Delta$ -Y conversion.

$R_N$  shown in Fig. 1 were given by following equations:

$$\begin{aligned}
 R_1 &= \Delta R_{\text{cell}} + \Delta R_{\text{collector}} \\
 R_2 &= \Delta R_{\text{cell}} // R_1 + \Delta R_{\text{collector}} \\
 &\vdots \\
 R_{N-1} &= \Delta R_{\text{cell}} // R_{N-2} + \Delta R_{\text{collector}} \\
 R_N &= \Delta R_{\text{cell}} // R_{N-1} + \Delta R_{\text{collector}}
 \end{aligned}
 \tag{1}$$

where // stands for parallel connection of the resistances.  $\Delta R_{\text{cell}}$  and  $\Delta R_{\text{collector}}$  are given as

$$\Delta R_{\text{cell}} = \frac{\text{ASR}}{\Delta A_{\text{cell}}}
 \tag{2}$$

and

$$\Delta R_{\text{collector}} = \frac{\Delta x}{A_{\text{collector}} \sigma},
 \tag{3}$$

where  $\Delta x$ , ASR,  $\Delta A_{\text{cell}}$ ,  $A_{\text{collector}}$  and  $\sigma$  are the width of sliced tube cell ( $\Delta x = L/N$ ), area specific resistance of the cell, the electrode area of the sliced tubular cell ( $\Delta A_{\text{cell}} = \pi d \Delta x$ ), the cross section area of the anode tube ( $A_{\text{collector}} = \pi t(d - t)$ ), and the conductivity of the anode tube in the reducing atmosphere [11], respectively. Note that value of ASR for the cell was chosen from experimental data with single terminal configuration just for reference, from the peak power density and the current of each temperature. The values of ASR were also used for the following model as well for comparison of two models.

In this calculation, current collecting resistance of the cathode part was assumed to be negligible. Efficiency loss was deter-

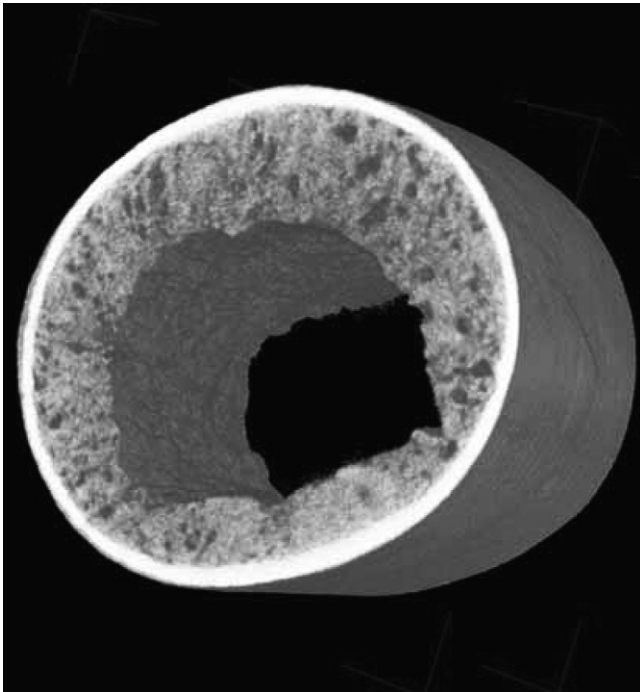


Fig. 3. Scan image of micro anode tube with dense electrolyte.

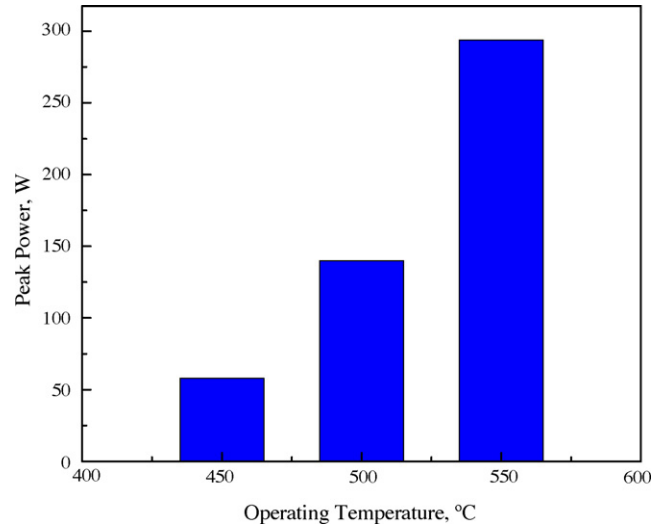


Fig. 4. Performance of single micro tubular SOFC (1 cm length 1.6 mm diameter) operated at 450–550 °C.

mined using a following relation,

$$\text{efficiency loss} = \frac{R_N - \text{ASR}/(\pi L d)}{R_N}
 \tag{4}$$

Here,  $R_N$  and  $\text{ASR}/(\pi L d)$  are total cell resistance including anode resistance, and true cell resistance, respectively.

### 3.2. Double terminal (DT) model

Fig. 2(a) shows the schematic image of double terminal current collecting method. Current collection from anode side is made from both terminals of the anode tube. The anode tube was divided into  $2^{N-1}$  and each of them was assigned to an equivalent circuit (highlighted in Fig. 2(b)).  $R_1, R_{a1}, R_2, R_{a2}, R_{a2,\text{new}}$ ,

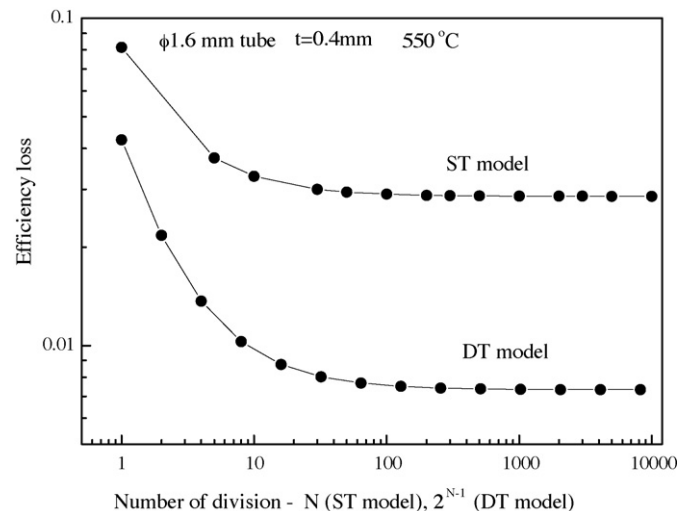


Fig. 5. Relationship between calculated efficiency loss and the number of division,  $N$  for the ST model and  $2^{N-1}$  for the DT model.

...,  $R_N$  shown in Fig. 2 were given by following equations:

$$\begin{aligned}
 R_1 &= \frac{ASR}{\Delta A_{\text{cell}}} \\
 R_{a,1} &= \frac{\Delta x}{A_{\text{collector}}\sigma} \\
 R_2 &= \frac{R_1^2}{2R_1 + R_{a,1}} \\
 R_{a,2} &= \frac{R_1 R_{a,1}}{2R_1 + R_{a,1}} \\
 R_{a2,\text{new}} &= 2R_{a,2} + R_{a,1} \\
 &\vdots \\
 R_{a,N} &= \frac{R_{N-1} R_{a,N-1,\text{new}}}{2R_{N-1} + R_{a,N-1,\text{new}}} \\
 R_N &= \frac{R_{N-1}^2}{2R_{N-1} + R_{a,N-1,\text{new}}}
 \end{aligned} \quad (5)$$

Total cell resistance including anode resistance can be written as

$$R_T = R_N + \frac{\sum R_{a,n}}{2} \quad (6)$$

In this calculation, the formula of  $\Delta$ -Y conversion (Fig. 2(c)) was used to simply the equivalent circuit. Efficiency loss was determined using a following relation:

$$\text{efficiency loss} = \frac{R_T - ASR/(\pi Ld)}{R_T} \quad (7)$$

where  $ASR/(\pi Ld)$  is true cell resistance.

#### 4. Results and discussion

Microstructure of the anode tube with an electrolyte layer was shown in Fig. 3. As can be seen, dense electrolyte was successfully realized on the surface of porous anode tube. The performance of the micro tube cell was shown in Fig. 4. The peak power of 58, 140, 294 mW obtained respectively at 450, 500

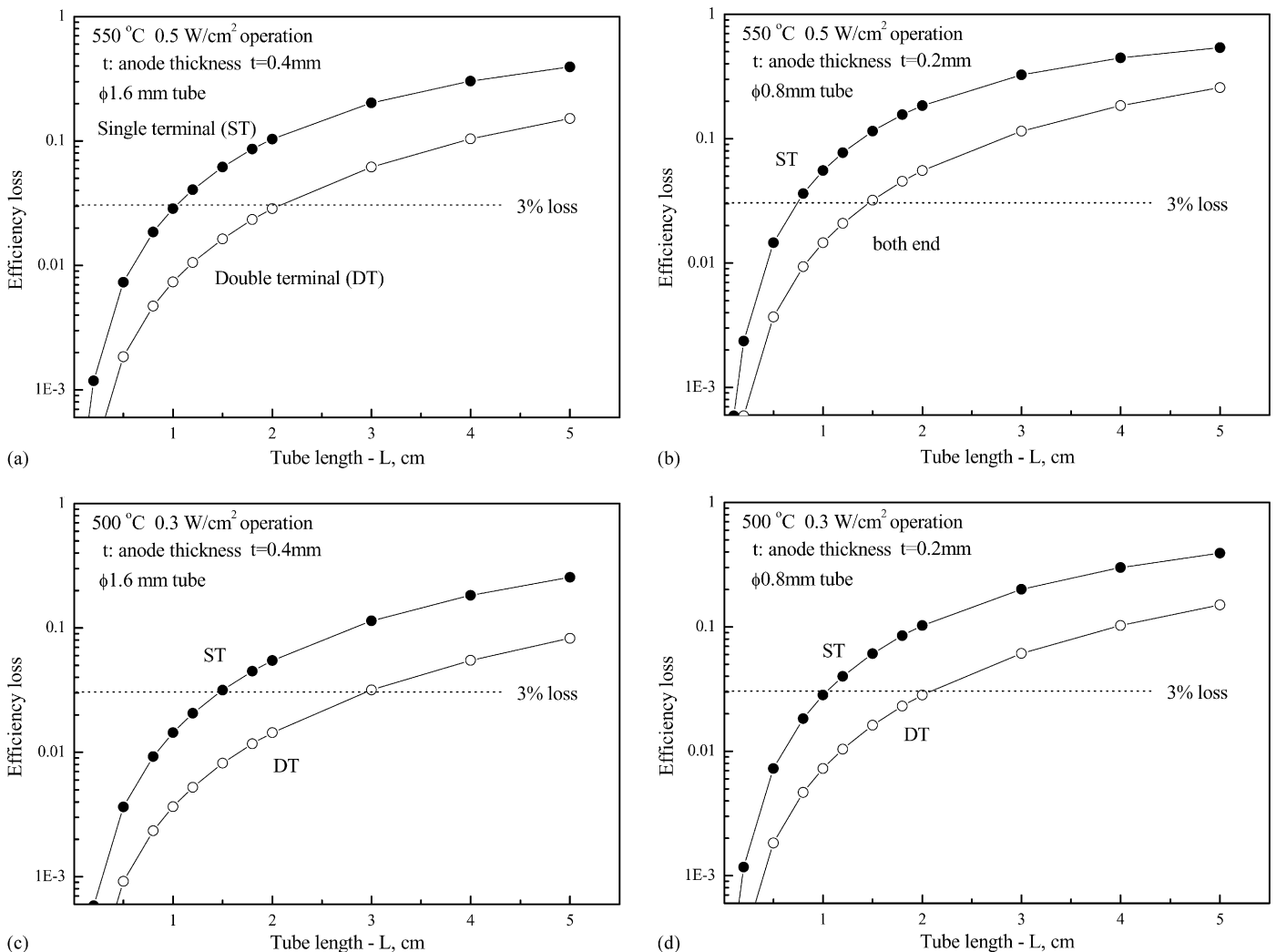


Fig. 6. Current efficiency loss as a function of anode tube length: (a) 1.6 mm diameter tube and (b) 0.8 mm diameter tube at 550 °C, (c) 1.6 mm diameter tube and (d) 0.8 mm diameter tube at 500 °C.

and 550 °C from the single cell with the length of 1 cm (cathode length = 7 mm). The open circuit voltages were dropped from 1.03 to 0.86 V as furnace temperature increased from 450 to 550 °C, which is usually explained by an increase of electronic conductivity at reducing atmosphere in ceria based electrolyte [12,13].

Fig. 5 shows the calculated efficiency loss in Eqs. (4) and (7) as a function of the number of division,  $N$  for the ST model and  $2^{N-1}$  for the DT model, respectively using the experimental data obtained at 550 °C for a 1.6 mm diameter tubular SOFC. It was shown that the efficiency loss saturated when the number of division is over 100 and thus,  $N=1000$  for the ST model and  $2^{N-1}=1024$  ( $N=11$ ) for the DT model were selected for further calculation.

Fig. 6 shows current efficiency loss as a function of anode tube length ( $L$ ) using the ST and DT models for (a) 1.6 mm and (b) 0.8 mm diameter tubes at 550 °C, (c) 1.6 mm and (d) 0.8 mm diameter tubes at 500 °C, respectively. A dashed line was drawn at 3% efficiency loss, which is considered to be the limit for practical use. As can be seen, the efficiency loss increased as the tube length increased due to increased anode resistance

as a current collector. In addition, the efficiency loss increased at higher operating temperature due to two reasons according to Eqs. (4) and (7); decreased cell resistance (increased power density) and increased anode tube (metallic) resistance.

Comparison of two models (ST and DT) clearly showed the advantage of the DT current collecting method. At each anode tube length, the efficiency loss obtained from DT model was about 2–4-fold lower than those of obtained from the ST model. The DT model becomes more effective when the operating temperature and the tube length increased.

Fig. 7 shows current efficiency loss as a function of anode tube thickness ( $t$ ) for 1 cm length cells (a) 1.6 mm and (b) 0.8 mm diameter tubes at 550 °C, (c) 1.6 mm and (d) 0.8 mm diameter tubes at 500 °C, respectively. The thickness of the anode tube does also strongly affect the current efficiency loss, especially for 0.8 mm diameter tubular SOFCs. As shown in Fig. 7, the DT current collecting method is also effective for reducing the loss caused by changing the thickness of the anode tube. It appeared that the efficiency loss was estimated over 3% at 550 °C operating temperature for actual experimental condition (1.6 mm diameter cell with  $t=0.4$  mm), while the loss can be negligi-

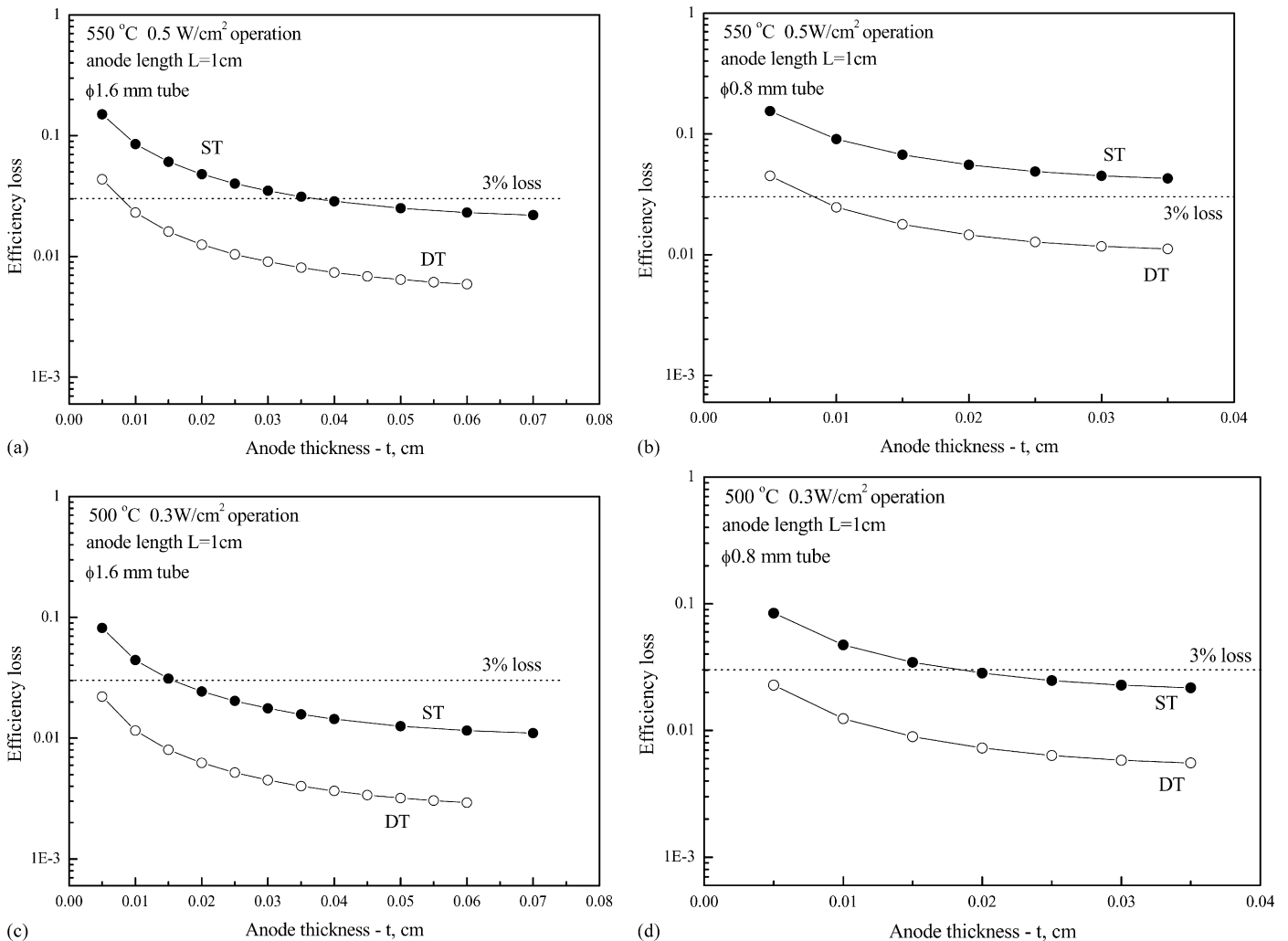


Fig. 7. Current efficiency loss as a function of anode tube thickness: (a) 1.6 mm diameter tube and (b) 0.8 mm diameter tube at 550 °C, (c) 1.6 mm diameter tube and (d) 0.8 mm diameter tube at 500 °C.

ble under 500 °C operating temperature using the DT current collecting method.

From these calculations, it was shown that followings can be effective to decrease the loss; (i) decrease operating temperature (ii) increase anode thickness (iii) increase conductivity of anode (less porosity) (iv) decrease electrode length. Since (i) and (iii) sacrifice the performance of the cell, (ii) and/or (iv) are considered to be more effective. Thus, it was shown that the selection of the anode tube length and current collecting method is very crucial to minimize the efficiency loss and this simulation can be useful and beneficial for designing the cell stacks and modules.

## 5. Summary

Micro tubular SOFCs with 1.6 mm diameter have been successfully fabricated using advanced ceramic processing technique. Typical electrolyte and electrode materials were selected, NiO–Gd doped ceria (GDC) as an anode (support tube), GDC as an electrolyte and (La, Sr)(Fe,Co)O<sub>3</sub> (LSCF)–GDC as a cathode. Note that the cells with 5 × 5 (25 cells) configurations can be placed in 1 cm<sup>3</sup> with the tube length of 1 cm (total electrode area ~10 cm<sup>2</sup>). The results show that the single tubular cell with 1.6 mm diameter and 1 cm length generated about 58, 140, 294 mW at 450, 500 and 550 °C with H<sub>2</sub> fuel. Two models for current collecting methods were proposed and used to estimate the current collecting model using the data obtained from actual SOFC measurement. The efficiency loss estimated from the double terminal model was about 2–4-fold lower than those of obtained from the single terminal model. Thus, the DT current collecting method was shown to be more effective for

higher operating temperature and the tube length. After all, selection of the length and thickness of the anode tube is crucial for designing micro tubular SOFC stack and these calculations are expected to provide optimum cell size to minimize efficiency loss.

## Acknowledgment

This work had been supported by NEDO, as part of the Advanced Ceramic Reactor Project.

## References

- [1] B.C.H. Steele, A. Heinzel, *Nature* 414 (2001) 345–352.
- [2] S.M. Haile, *Acta Materialia* 51 (2003) 5982–6000.
- [3] Z. Shao, S.M. Haile, *Nature* 431 (2004) 170–173.
- [4] T. Hibino, A. Hashimoto, K. Asano, M. Yano, M. Suzuki, M. Sano, *Electrochem. Solid-State Lett.* 5 (11) (2002) A242–A244.
- [5] J. Yan, H. Matsumoto, M. Enoki, T. Ishihara, *Electrochem. Solid-State Lett.* 8 (8) (2005) A389–A391.
- [6] B.C.H. Steele, *Solid State Ionics* 129 (2000) 95–110.
- [7] H. Yokokawa, T. Horita, N. Sakai, K. Yamaji, M.E. Brito, Y.-P. Xiong, H. Kishimoto, *Solid State Ionics* 174 (2004) 205–221.
- [8] N.M. Sammes, Y. Du, R. Bove, *J. Power Sources* 145 (2005) 428–434.
- [9] K. Kendall, M. Palin, *J. Power Sources* 71 (1998) 268–270.
- [10] K. Yashiro, N. Yamada, T. Kawada, J. Hong, A. Kaimai, Y. Nigara, J. Mizusaki, *Electrochemistry* 70 (12) (2002) 958–960.
- [11] T. Suzuki, T. Yamaguchi, Y. Fujishiro, M. Awano, *J. Power Sources* 160 (2006) 73–77.
- [12] D. Hirabayashi, A. Tomita, T. Hibino, M. Nagao, M. Sano., *Electrochem. Solid-State Lett.* 7 (10) (2004) A318–A320.
- [13] D. Hirabayashi, A. Tomita, S. Teranishi, T. Hibino, M. Sano., *Solid State Ionics* 176 (10) (2005) 881–887.